Pattern-Search-Based Nonconvex Cooperative Sensing in Multiband Cognitive Radio Systems

Ahmed Shaharyar Khwaja, Muhammad Naeem, and Alagan Anpalagan

***Abstract*—In this paper, a pattern search (PS)-based solution is proposed for nonconvex multiband cooperative sensing (NCMCS) problem in cognitive radio systems. This problem consists of maximizing cumulative throughput subject to constraints on cumulative interference, probability of detection, and probability of false alarm. Initially in existing literature, this problem was solved under constraints that make it convex. However, removing the conditions for convexity and solving the NCMCS problem have been shown to improve performance. A two-step PS-based solution is presented: The first step uses uniformly distributed random sets of input points to find a solution. The set of points that gives the maximum throughput is chosen as input to the PS algorithm. Numerical examples show the improvement of the proposed method over existing genetic-algorithm-based solution, as well as PS-algorithm-based solution that uses a single set of random points as inputs. The proposed two-step solution gives higher cumulative throughput and is not sensitive to the choice of input, unlike the PS-based solution using a single set of random points as input.**

***Index Terms*—Cognitive radio (CR), collaborative sensing, global optimization, nonconvexity, pattern search (PS).**

NOTATIONS AND SYMBOLS

K	Number of subchannels.
M	Number of users.
N	Number of channel measurements.
$\boldsymbol{w}$	Weight factor vector.
$\boldsymbol{\gamma}$	Threshold vector.
$R(\boldsymbol{w}, \boldsymbol{\gamma})$	Total throughput.
$I(\boldsymbol{w}, \boldsymbol{\gamma})$	Cumulative interference.
$\boldsymbol{r}$	Achievable output vector.
$P_f(\boldsymbol{w}_k, \gamma_k)$	Probability of false alarm for the kth subband.
$P_d(\boldsymbol{w}_k, \gamma_k)$	Probability of detection for the kth subband.
ε	Maximum interference limit.
α	Limit for probability of interference.
β	Limit for probability of detection.
$\boldsymbol{c}$	Measure of cost caused by transmitting in the band vector.
$\boldsymbol{\mu}_{0,k}$	Mean vector in the presence of noise for the kth subband.
$\boldsymbol{\mu}_{1,k}$	Mean vector in the presence of signal and noise for the kth subband.
$\boldsymbol{\Sigma}_{0,k}$	Covariance vector in the presence of noise for the kth subband.
$Q_f(.)$	Q function.
SNR	Signal-to-noise ratio.
N_s	Number of sets of input points used in the first stage of the proposed algorithm.
$\boldsymbol{\Sigma}_{1,k}$	Covariance vector in the presence of signal and noise for the kth subband.
p_s	Signal power.
σ_v^2	Noise power.
NCMCS	Nonconvex multiband cooperative sensing.
T_k^i	Energy sensed at the kth subband of the ith CR.
z_k	Result of combination of weighted sensed energies for kth subband.
$x_k^i(n)$	nth measurement at the kth subband of the ith CR.
$\boldsymbol{B}$	Basis matrix.
$\boldsymbol{C}$	Generating matrix.
$\boldsymbol{M}$	Components of the generating matrix.
$\boldsymbol{I}$	Identity matrix.
$\boldsymbol{P}_k$	Pattern matrix at iteration k.
$\boldsymbol{p}_k^i$	ith column of $\boldsymbol{P}_k$.
ρ_k	Difference between two function evaluations.
δ_k	Step length.
$\boldsymbol{\varrho}$	Unknown parameter to be optimized, contains both threshold and weight vectors.
$\boldsymbol{\varrho}_k$	kth unknown parameter to be optimized.
$\overline{\boldsymbol{c}}(\boldsymbol{\varrho})$	Constraint vector.
$\overline{c}_k(\boldsymbol{\varrho})$	Constraint value.
σ	Augmented Lagrangian parameter.
$\boldsymbol{\lambda}$	Lagrangian parameter.
ς	Slack variable.

In this paper, $\mathcal{R}$ represents real numbers, $\mathcal{Q}$ represents rational numbers, and $\mathcal{Z}$ represents integers. Symbols $\boldsymbol{X}$, $\boldsymbol{x}$, and x represent a matrix, a vector, and an element of a vector, respectively. When $x_i \geq 0$ for all components i of a vector $\boldsymbol{x}$, $\boldsymbol{x} \geq 0$ is used. $\boldsymbol{x}^T$ means transpose of $\boldsymbol{x}$.

I. INTRODUCTION

THE congestion of wireless spectrum due to continuously increasing number of wireless users and services requires efforts to design efficient wireless systems. Traditional fixed wireless spectrum assignment consists of assigning selected frequency bands to different users, known as licensed users (LUs) and/or primary users (PUs). This assignment strategy leads to inefficient utilization as some bands may be in use

Manuscript received July 23, 2013; revised December 30, 2013; accepted January 2, 2014. Date of publication February 28, 2014; date of current version May 30, 2016.

A. S. Khwaja and A. Anpalagan are with the WINCORE Lab, Department of Electrical and Computer Engineering, Ryerson University, Toronto, ON M5B 2K3, Canada.

M. Naeem is with the Department of Electrical Engineering, COMSATS Institute of Information Technology, Wah Cantt, Pakistan, and also with the WINCORE Lab, Ryerson University, Toronto, ON M5B 2K3, Canada.

Digital Object Identifier 10.1109/JSYST.2014.2305871

all the time, whereas the others may be intermittently used [1]. Cognitive radio (CR) [2] provides a way to improve the wireless spectrum utilization efficiency and has been successfully used in many fields such as communications [3], [4], health [5], and smart grid [6].

CR can be described as a feedback wireless communication system that is "aware" of its surroundings. It can learn from the surroundings and adapt to statistical variations in the surroundings [2]. It has two primary objectives: to achieve highly reliable communication and to enable efficient utilization of the radio spectrum. These objectives are achieved by CRs by allowing different unlicensed users (ULUs) and/or secondary users (SUs) to share the band of an LU when it is not in use. This requires spectrum sensing and is carried out by minimizing the interference caused by the ULUs at the receivers of LUs.

Spectrum sensing dynamically identifies parts of the spectrum that are not in use by any PU at a particular time. There are various kinds of spectrum sensing algorithms [8]–[12]. The energy detection algorithm given in [10]–[12] is normally chosen as it is simple, fast, and does not require any prior information. However, it is not robust to noise uncertainty, and one of the major problems that this algorithm encounters is the hidden terminal problem [15]. This problem occurs when there is shadowing or the transmitted signal is degraded due to high path loss while an LU is active [13]. As a result, when the SNR of the channel falls below a certain threshold, ULUs cannot independently decide whether a PU is present or not.

The hidden terminal problem can be dealt with using cooperative sensing [14]. It consists of a combination of local spectrum information from multiple CR users for LU detection [11]. In this case, the combined/cooperative decision can overcome the deficiency of individual information at each CR user and improve performance in the presence of multipath fading and shadowing. Different approaches can be found in literature to implement the cooperative sensing: In [16], every SU makes a decision and sends this decision as a single bit to the secondary base units for fusion. In [17], the Dempster–Shafer theory is used to combine different sensing decisions from each CR. Linear statistics combination (LSC) technique is proposed in [18]. It combines the locally sensed power levels, instead of the binary decisions, and performs a unique test decision; LSCs have been demonstrated to enhance the performance noticeably [19].

Originally, the cooperative sensing algorithms were proposed for a single band only [19], where a bandpass filter (BPF) was needed to extract the target signal. This type of sensing limits the time during which the SUs can transmit, therefore reducing the system efficiency [20]. Extending the detector that only extracts a narrow-band spectrum, for wideband spectrum sensing, requires a tunable BPF at the radio frequency front end, which can be used to scan one band at a time [21]. This mechanism is slow and inflexible [19]. In [22] and [23], wavelets were used to enable wideband spectrum sensing; however, these references do not deal with cooperative multiband spectrum sensing. To improve the ability of a CR to process multiple bands jointly, efficient wideband sensing algorithms are a necessity.

A block diagram of a wideband cooperative sensing CR system is shown in Fig. 1, where the dotted box deals with the sensing process. It can be seen that this block takes input from

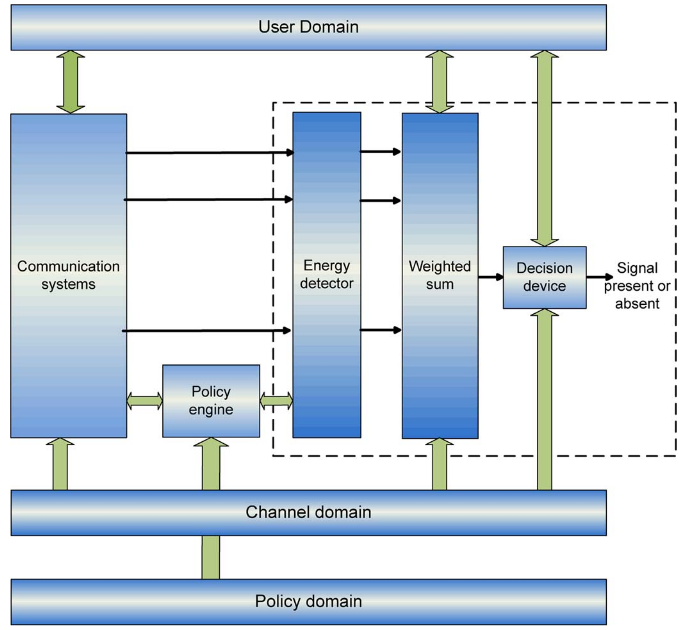

Fig. 1. Block diagram of cooperative sensing CR system.

policy, channel, and user domains about regulations, quality of link, characteristics of wireless signals, user's quality of service requirements, etc. Based on this input, the received multiband signal from receivers is first detected using energy detectors. The detected signal is then used in a weighted sum to combine all the energy signals. This weighted sum is followed by a decision block that decides if a signal from a PU is present or not.

Reference [18] introduced multiband cooperative sensing that is formulated as an optimization problem. It consists of maximizing the cumulative throughput subject to the following three constraints.

- Minimizing the cumulative interference to the LUs over all the bands. The interference is bounded by an upper threshold.
- Minimizing the probability of false alarm, i.e., P_f, which indicates the presence of an LU, although the band is free. This probability is bounded by an upper threshold.
- Maximizing the probability of detection, i.e., P_d, which means a CR indicates the presence of an LU correctly. This probability is bounded by a lower threshold.

The aforementioned optimization problem is nonconvex. This means that a solution can be a local optimum point, instead of a global point [24]. The authors in [18] showed that under certain constraints on P_f and P_d, the problem becomes a convex optimization problem. They solved this problem using interior-point method. In [25] and [26], the authors solved this convex problem using artificial immune system and Taguchi method, respectively. However, it has been shown in [27] that these constraints limit the performance of the system. Consequently, the authors used genetic algorithm (GA) to deal with the nonconvex optimization problem and showed that a higher throughput versus interference can be achieved. A comparison of the different references is presented in Table I.

In this paper, a pattern search (PS) algorithm [28] based solution is proposed for solving the NCMCS problem. PS are a class of direct search methods [7] for nonlinear optimization.

TABLE I
COMPARISON OF DIFFERENT REFERENCES

References	Convex	Non-convex	Algorithm	Remarks
[21]	N/A	N/A	N/A	Tunable narrow-band band pass filter is used to sense one band at a time, no collaborative sensing over all the bands is used
[22], [23]	N/A	N/A	N/A	Uses Wavelet transforms for multi-band spectrum sensing, no collaborative sensing over all the bands is used
[18]	Yes	No	Interior-point method	Can only be applied to multi-band cooperative sensing case, only works in the convex case
[27]	Yes	Yes	Genetic algorithm	Can deal with both convex and non-convex multi-band cooperative sensing cases, not proved to be globally convergent, requires more function evaluations
[25]	Yes	No	Artificial immune system	Can deal with convex multi-band cooperative sensing, only applied to convex case
[26]	Yes	No	Taguchi method	Can deal with convex multi-band cooperative sensing, only applied to convex case

They are selected in this paper as they are probably convergent. They are also simple to implement as they do not require a direct estimate of the derivative, and unlike other heuristic algorithms, they can adapt to both global and local search. The PS algorithm aims to find the solution by evaluating the objective function over a suitable set of trial points iteratively. This way, it tries to overcome the lack of information on the derivatives by investigating the behavior of the objective function in a neighborhood of the current iteration. However, PS is sensitive to initial points and can have irregular performance, as shown in this paper. To deal with this issue, a two-step optimization procedure is proposed.

- A modified PS algorithm based on multiple-input initialization is proposed, where a number of uniformly distributed random sets of points are used to solve the optimization problem.
- The set of points that gives the maximum value of the objective function is chosen as the initial point for the PS algorithm.

Numerical examples show that the two-step procedure greatly improves performance compared with existing GA and using PS with random inputs only. The rest of this paper is organized as follows: The system model is presented in Section II. In Section III, the PS method and the proposed solution are described. Simulation results are presented in Section IV, and this paper is concluded in Section V.

II. Problem Formulation of Collaborative Multiband Sensing

Let M be the number of CRs, K be the number of subchannels/subbands, and N be the number of channel measurements. The nth measurement at the kth subband of the ith CR is denoted by $x_{k,i}(n)$. Let the energy sensed at the kth subband of the ith CR be defined as [19]

$$T_{k,i} = \sum_{n=1}^{N} |x_{k,i}(n)|^2 . \tag{1}$$

The energy results for the kth subband and M CRs are given by a vector $\boldsymbol{y}_k$ as follows:

$$\boldsymbol{y}_k = [T_{k,1}, T_{k,2}, \ldots, T_{k,M}]. \tag{2}$$

These results are linearly combined as follows [37]:

$$z_k = \boldsymbol{w}_k \boldsymbol{y}_k^T \tag{3}$$

where the weight vector $\boldsymbol{w}_k$ is defined as

$$\boldsymbol{w}_k = [w_{k,1}, w_{k,2}, \ldots, w_{k,M}]. \tag{4}$$

An energy detector is used by the SU for spectrum sharing [29], [37]: z_k is compared with a threshold γ_k to decide the presence or the absence of signal from a PU in the kth subband. A summary of this process is given in Fig. 2.

Furthermore, $z_k \sim \mathcal{N}(\boldsymbol{w}_k \boldsymbol{\mu}_{0,k}, \boldsymbol{w}_k \boldsymbol{\Sigma}_{0,k} \boldsymbol{w}_k^T)$ in the presence of noise, and $z_k \sim \mathcal{N}(\boldsymbol{w}_k \boldsymbol{\mu}_{1,k}, \boldsymbol{w}_k \boldsymbol{\Sigma}_{1,k} \boldsymbol{w}_k^T)$ in the presence of both signal and noise. The mean vectors in the presence of noise and in the presence of both signal and noise are denoted by $\boldsymbol{\mu}_{0,k}$ and $\boldsymbol{\mu}_{1,k}$, respectively. The covariance matrices in the presence of noise and in the presence of both signal and noise are denoted by $\boldsymbol{\Sigma}_{0,k}$ and $\boldsymbol{\Sigma}_{1,k}$, respectively. They are defined as [19]

$$\boldsymbol{\mu}_{0,k} = N\left[\sigma_{v_1}^2, \sigma_{v_2}^2, \ldots, \sigma_{v_M}^2\right]^T \tag{5}$$

$$\boldsymbol{\mu}_{1,k} = N\left[\sigma_{v_1}^2 + p_{s_1}, \sigma_{v_2}^2 + p_{s_2}, \ldots, \sigma_{v_M}^2 + p_{s_M}\right]^T \tag{6}$$

$$\boldsymbol{\Sigma}_{0,k} = 2N \begin{bmatrix} \sigma_{v_1}^4 & & & \\ & \cdot & & \\ & & \cdot & \\ & & & \sigma_{v_M}^4 \end{bmatrix} \tag{7}$$

$$\boldsymbol{\Sigma}_{1,k} = 2N \begin{bmatrix} \sigma_{v_1}^2\left(\sigma_{v_1}^2 + p_{s_1}\right) & & & \\ & \cdot & & \\ & & \cdot & \\ & & & \sigma_{v_M}^2\left(\sigma_{v_M}^2 + p_{s_M}\right) \end{bmatrix} \tag{8}$$

where σ_v^2 is the variance of noise, and p_{s_m} is the signal power at the mth CR. The probabilities of detection and interference are given as [37]

$$P_d(\boldsymbol{w}_k, \gamma_k) = Q_f\left(\frac{\gamma_k - \boldsymbol{w}_k \boldsymbol{\mu}_{1,k}}{\sqrt{\boldsymbol{w}_k \boldsymbol{\Sigma}_{1,k} \boldsymbol{w}_k^T}}\right) \tag{9}$$

$$P_f(\boldsymbol{w}_k, \gamma_k) = Q_f\left(\frac{\gamma_k - \boldsymbol{w}_k \boldsymbol{\mu}_{0,k}}{\sqrt{\boldsymbol{w}_k \boldsymbol{\Sigma}_{0,k} \boldsymbol{w}_k^T}}\right). \tag{10}$$

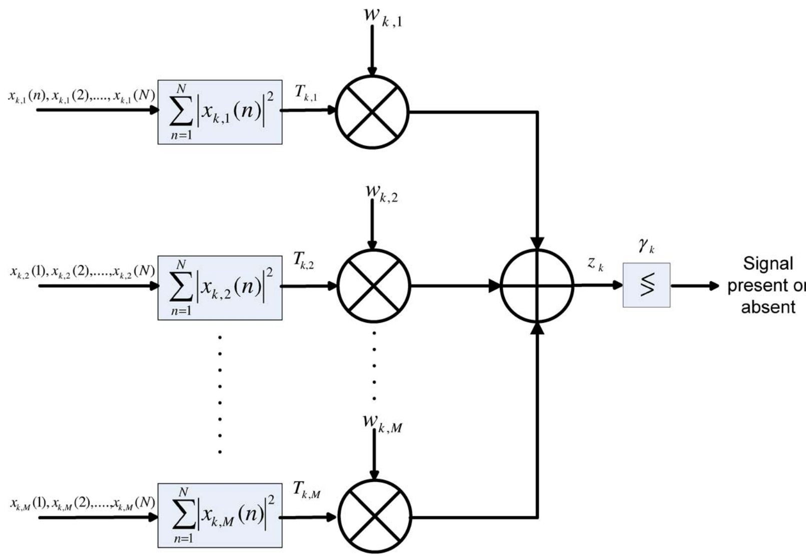

Fig. 2. Multiband cooperative CR system.

The weights and thresholds are the variables that can be optimized. As a result, the problem of multiband cooperative sensing can be posed as the maximization of spectrum efficiency that is defined as

$$\begin{aligned}
&\min_{\boldsymbol{w},\gamma} -R(\boldsymbol{w},\boldsymbol{\gamma})\\
&\text{subject to}\\
&I(\boldsymbol{w},\boldsymbol{\gamma}) \leq \varepsilon\\
&1-\boldsymbol{P}_d(\boldsymbol{w},\boldsymbol{\gamma}) \leq \alpha\\
&1-\boldsymbol{P}_f(\boldsymbol{w},\boldsymbol{\gamma}) \geq \beta\\
&0 \leq \boldsymbol{w} \leq 1\\
&\boldsymbol{\gamma}_{\min} \leq \boldsymbol{\gamma} \leq \boldsymbol{\gamma}_{\max}
\end{aligned} \tag{11}$$

where

$$R(\boldsymbol{w},\boldsymbol{\gamma}) = \boldsymbol{r}\left[1-\boldsymbol{P}_f(\boldsymbol{w},\boldsymbol{\gamma})\right]^T \tag{12}$$

is the cumulative throughput, and $\boldsymbol{r} = [r_1, r_2, \ldots, r_K]^T$ is the maximum throughput available from a band. Thus

$$I(\boldsymbol{w},\boldsymbol{\gamma}) = \boldsymbol{c}\left[1-\boldsymbol{P}_d(\boldsymbol{w},\boldsymbol{\gamma})\right]^T \tag{13}$$

is the cumulative interference, and $\boldsymbol{c} = [c_1, c_2, \ldots, c_K]^T$ is the cost of transmitting in the band when a PU is using it. The threshold limits $\boldsymbol{\gamma}_{\min}$ and $\boldsymbol{\gamma}_{\max}$ can be calculated as described in [27]. In addition

$$\boldsymbol{w} = [\boldsymbol{w}_1, \boldsymbol{w}_2, \ldots, \boldsymbol{w}_K] \tag{14}$$

$$\boldsymbol{\gamma} = [\gamma_1, \gamma_2, \ldots, \gamma_K] \tag{15}$$

are the weight and threshold vectors, respectively. The vectors of probability of detection and probability of false alarm are given as

$$\boldsymbol{P}_f(\boldsymbol{w},\boldsymbol{\gamma}) = [P_f(\boldsymbol{w}_1,\gamma_1), P_f(\boldsymbol{w}_2,\gamma_2), \ldots, P_f(\boldsymbol{w}_K,\gamma_K)] \tag{16}$$

$$\boldsymbol{P}_d(\boldsymbol{w},\boldsymbol{\gamma}) = [P_d(\boldsymbol{w}_1,\gamma_1), P_d(\boldsymbol{w}_2,\gamma_2), \ldots, P_d(\boldsymbol{w}_K,\gamma_K)]. \tag{17}$$

The preceding problem is convex only for $\alpha \leq 0.5$, $\beta \geq 0.5$. For other values of α and β, the problem is nonconvex and can be solved using nonconvex optimization techniques. There are many evolutionary algorithms for solving the nonconvex optimization problem. Among these algorithms, it has been shown that the particle swarm optimization (PSO) algorithm can outperform other evolutionary algorithms such as GA, memetic algorithm, ant colony optimization, and shuffled frog leaping optimization algorithms [30]. PS is another optimization technique [31] and has been shown to have superior performance even compared with PSO for both simple and complicated problems [32]. In addition, unlike GA and PSO, PS can adapt to global and local search [33] and requires very few hand-tuned input parameters. These parameters can affect the performance significantly, particularly in both conventional and improved versions of GA [34]. The PS algorithm that carries out constraint satisfaction via augmented Lagrangian method [35] is described in the next section.

III. Solution of the Optimization Problem

A. GA

The PS algorithm is simple to implement as it does not calculate any specific information about the gradient. It is shown to be convergent in [36]. A block diagram of the PS algorithm is given in Fig. 3. It is shown in the figure that the idea of the PS algorithm is based on two main steps: exploratory step and updating step. In the exploratory step, a collection of points, which is known as mesh, is selected around the current points. The current points can be initial points provided at the start of the algorithm or points from a previous step. Each set of points in the mesh is multiplied by a given step size and then added to the current points. The objective function is evaluated at the resulting points. If the new value of the objective function at a step shows improvement over the previous points, the exploratory step is considered successful. Otherwise, the step is considered as unsuccessful, and the next set of points in the mesh is used to evaluate the objective function.

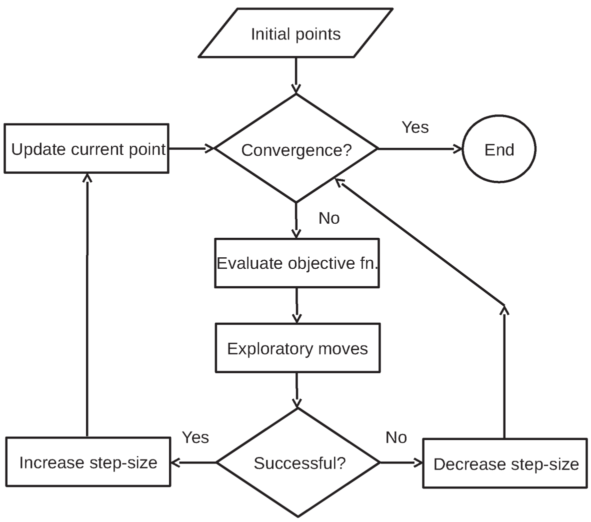

Fig. 3. Flowchart of PS algorithm.

The updating step is used to select the step size for the next exploratory step. If the pattern move was successful, the step size is increased, and the resulting step size is used for the next exploratory step. If there was no improvement with any of the sets in the mesh, the step size is decreased for the new exploratory step.

For a solution to the problem

$$\min_{\boldsymbol{x}} f(\boldsymbol{x}) \tag{18}$$

the PS algorithm is described by Algorithm 1.

Algorithm 1: General PS algorithm

$l \leftarrow 1$
Initialization: *Generate $\boldsymbol{x}_1$ randomly between a lower upper bound*
while $l \leq MaxIter$
  Check for convergence
  Evaluate the objective function $f(\boldsymbol{x}_l)$
  Determine a trial step $\boldsymbol{s}_l$ using exploratory moves algorithm
  $\rho_l \leftarrow f(\boldsymbol{x}_l) - f(\boldsymbol{x}_l + \boldsymbol{s}_l)$
  If $\rho_l > 0$, $\boldsymbol{x}_{l+1} \leftarrow \boldsymbol{x}_l + \boldsymbol{s}_l$. Otherwise, $\boldsymbol{x}_{l+1} \leftarrow \boldsymbol{x}_l$
  Update Δ_l
  $l \leftarrow l + 1$
end while

In the following, each step of the algorithm is described.

Check for Convergence: The convergence is verified by checking if the change over the last evaluations of the objective function is smaller than a threshold. This means that the iterations are not leading to any improvement of the solution, and hence, the algorithm should be stopped.

Determine a Trial Step $\boldsymbol{s}_l$: To determine a trial step $\boldsymbol{s}_l$ at iteration l, the pattern and mesh need to be defined.

- Pattern definition: To define a pattern, two components are needed, namely, a basis matrix and a generating matrix. The basis matrix can be any nonsingular matrix $\boldsymbol{B} \in R^{n\times n}$. The generating matrix is a matrix $\boldsymbol{C}_k \in Z^{n\times p}, p > n$. It is partitioned into components, $\boldsymbol{C}_l = [\boldsymbol{M}_l - \boldsymbol{M}_l]$, where $\boldsymbol{M}_l \in \boldsymbol{M} \subset Z^{n\times n}$. A pattern $\boldsymbol{p}_l^i$ is then defined by the columns of the matrix $\boldsymbol{P}_l = \boldsymbol{B}\boldsymbol{C}_k$, where $\boldsymbol{P}_l = [\boldsymbol{p}_l^1, \ldots, \boldsymbol{p}_l^{\widetilde{p}}]$.
- Mesh definition: Given a step size $\Delta_l \in \mathcal{R}$, $\Delta_l > 0$, a trial step $\boldsymbol{s}_l^i$ can be any vector of the form $\boldsymbol{s}_l^i = \Delta_l \boldsymbol{p}_l^i$. Note that $\boldsymbol{p}_l^i$ determines the direction of the step, whereas Δ_l serves as the step length parameter. At iteration l, a set of trial points is defined as $\boldsymbol{x}_l^i = \boldsymbol{x}_l + \boldsymbol{s}_l^i$, where $\boldsymbol{x}_l$ is the current set.
- Exploratory moves: The exploratory moves are sequentially executed to select a trial step. The selection of the next trial step is based on the success or failure of the previous trial step. If the previous trial step leads to a decrease in objective function, then the trial step is retained. Otherwise, the trial step is decreased.

Updating: The aim of the updating algorithm for Δ_l is to force $f(\boldsymbol{x}_l^i) < f(\boldsymbol{x}_l)$. An iteration with $f(\boldsymbol{x}_l^i) < f(\boldsymbol{x}_l)$ is successful; otherwise, the iteration is unsuccessful. If the iteration is successful, the trial step size is increased by a factor λ. Otherwise, it is decreased by a factor θ.

B. Proposed Solution With PS Algorithm

Coordinate search is defined so that the basis matrix is the identity matrix, i.e., $\boldsymbol{B} = \boldsymbol{I}$. The generating matrix for coordinate search is fixed across all iterations of the method, i.e., $\boldsymbol{C}_l = \boldsymbol{C}$, $\forall l$. The generating matrix is partitioned into two components: $\boldsymbol{C} = [\boldsymbol{I}, -\boldsymbol{I}], \boldsymbol{I} \in Z^{n\times n}$, where $\boldsymbol{I}$ is an identity matrix, e.g., if $n = 4$, $\boldsymbol{C}$ can be defined as

$$\boldsymbol{C} = \begin{bmatrix} 1 & 0 & 0 & 0 & -1 & 0 & 0 & 0 \\ 0 & 1 & 0 & 0 & 0 & -1 & 0 & 0 \\ 0 & 0 & 1 & 0 & 0 & 0 & -1 & 0 \\ 0 & 0 & 0 & 1 & 0 & 0 & 0 & -1 \end{bmatrix}. \tag{19}$$

1) Rewriting of the Problem: In order to apply PS to collaborative multiband sensing problem, the variables to be optimized are rewritten as follows:

$$\boldsymbol{\varrho} = [\boldsymbol{w}, \boldsymbol{\gamma}] \tag{20}$$

such that

$$\boldsymbol{\varrho} = [\boldsymbol{\varrho}_1, \boldsymbol{\varrho}_2, \ldots, \boldsymbol{\varrho}_K] \tag{21}$$

where $\boldsymbol{\varrho}_k = [\boldsymbol{w}_k, \boldsymbol{\gamma}_k]$. The optimization problem can be rewritten as

$$\begin{aligned} &\min_{\boldsymbol{\varrho}} -R(\boldsymbol{\varrho}) \\ &\text{subject to} \\ &\overline{\boldsymbol{c}}(\boldsymbol{\varrho}) \leq 0 \\ &0 \leq \boldsymbol{\varrho}_1, \boldsymbol{\varrho}_3, \boldsymbol{\varrho}_5, \ldots, \boldsymbol{\varrho}_{K-1} \leq 1 \\ &\gamma_{\min} \leq \boldsymbol{\varrho}_2, \boldsymbol{\varrho}_4, \boldsymbol{\varrho}_6, \ldots, \boldsymbol{\varrho}_K \leq \gamma_{\max} \end{aligned} \tag{22}$$

where

$$\begin{aligned} \bar{\boldsymbol{c}}(\boldsymbol{\varrho}) &= [\bar{c}_1(\boldsymbol{\varrho}), \bar{c}_2(\boldsymbol{\varrho}), \ldots, \bar{c}_{2K+1}(\boldsymbol{\varrho})] \\ \bar{c}_1(\boldsymbol{\varrho}) &= I(\boldsymbol{\varrho}) - \varepsilon \\ \bar{c}_2(\boldsymbol{\varrho}) &= [1 - \boldsymbol{P}_d(\varrho_1) - \alpha] \\ \bar{c}_3(\boldsymbol{\varrho}) &= [1 - \boldsymbol{P}_d(\varrho_2) - \alpha] \\ &\;\;\vdots \\ \bar{c}_{K+1}(\boldsymbol{\varrho}) &= [1 - \boldsymbol{P}_d(\varrho_K) - \alpha] \\ \bar{c}_{K+2}(\boldsymbol{\varrho}) &= [\beta - 1 + \boldsymbol{P}_f(\varrho_1)] \\ \bar{c}_{K+3}(\boldsymbol{\varrho}) &= [\beta - 1 + \boldsymbol{P}_f(\varrho_2)] \\ &\;\;\vdots \\ \bar{c}_{2K+1}(\boldsymbol{\varrho}) &= [\beta - 1 + \boldsymbol{P}_f(\varrho_K)] \end{aligned} \tag{23}$$

2) Constraint Satisfaction via Augmented Lagrangian: The constraint functions are checked via augmented Lagrangian method. As a first step, an inequality constraint $\bar{c}_i(\boldsymbol{x}) \le 0$ is transformed into the equality constraint $\bar{c}_m(\boldsymbol{x}) + \varsigma_m^2 = 0$ by using a squared slack variable ς_m^2. Let λ_m be the multiplier associated with the mth constraint, then the augmented Lagrangian function for the equality constrained equation becomes

$$L_a(\boldsymbol{\varrho}, \boldsymbol{\varsigma}, \boldsymbol{\lambda}; \sigma) = -R(\boldsymbol{\varrho}) + \sum_m \lambda_m \left(\bar{c}_m(\boldsymbol{\varrho}) + \varsigma_m^2\right) + \frac{1}{\sigma} \sum_m \lambda_m \left(\bar{c}_m(\boldsymbol{\varrho}) + \varsigma_m^2\right)^2 \tag{24}$$

where σ is a penalty parameter, and $\boldsymbol{\lambda} = [\lambda_1, \lambda_2, \ldots, \lambda_{2K+1}]$. Equation (24) can be minimized with respect to $\boldsymbol{\varsigma}$ in a closed form as follows.

1) Carry out the derivative of (24) with respect to $\boldsymbol{\varsigma}_m^2$, i.e.,

$$\frac{d^2 L_a(\boldsymbol{\varrho}, \boldsymbol{\varsigma}, \boldsymbol{\lambda}; \sigma)}{d\boldsymbol{\varsigma}_m^2} = \lambda_m + \frac{2\bar{c}_m(\boldsymbol{\varrho})}{\sigma} + \frac{2\varsigma_m^2}{\sigma} \tag{25}$$

and equate it to 0, which leads to

$$-\boldsymbol{\varsigma}_m^2 = \frac{\sigma\lambda_m}{2} + \bar{c}_m(\boldsymbol{\varrho}). \tag{26}$$

2) As a result, $\min_{\boldsymbol{\varsigma}} L_a(\boldsymbol{\varrho}, \boldsymbol{\varsigma}, \boldsymbol{\lambda}; \sigma)$ can be solved in a closed form as follows:

$$\min_{\boldsymbol{\varsigma}} L_a(\boldsymbol{\varrho}, \boldsymbol{\varsigma}, \boldsymbol{\lambda}; \sigma) = \begin{cases} \frac{-\sigma\lambda_m}{2} + \bar{c}_m(\boldsymbol{\varrho}), & \text{if } \bar{c}_m(\boldsymbol{\varrho}) < \frac{-\sigma\lambda_m}{2} \\ 0, & \text{otherwise.} \end{cases}$$

3) Consequently, the expression in (24) can be simplified as follows:

$$\bar{c}_m(\boldsymbol{\varrho}) + \varsigma_m^2 = \begin{cases} \frac{-\sigma\lambda_m}{2}, & \text{if } \bar{c}_m(\boldsymbol{\varrho}) < \frac{-\sigma\lambda_m}{2} \\ \bar{c}_m(\boldsymbol{\varrho}), & \text{otherwise.} \end{cases}$$

4) As a result, (24) can be rewritten as

$$L_a(\boldsymbol{\varrho}, \boldsymbol{\lambda}; \sigma) = \begin{cases} -R(\boldsymbol{\varrho}) - \frac{\sigma\boldsymbol{\lambda}\boldsymbol{\lambda}^T}{4} & \text{, if } \bar{\boldsymbol{c}}(\boldsymbol{\varrho}) < -\frac{\sigma\boldsymbol{\lambda}}{2} \\ -R(\boldsymbol{\varrho}) + \boldsymbol{\lambda}\bar{\boldsymbol{c}}^T(\boldsymbol{\varrho}) + \frac{1}{\sigma}\left\|\bar{\boldsymbol{c}}(\boldsymbol{\varrho})\right\|^2 & \text{, otherwise.} \end{cases} \tag{27}$$

The PS algorithm for solving the NCMCS problem along with constraint satisfaction is summarized in Algorithm 2.

TABLE II
COMPARISON OF DIFFERENT TECHNIQUES

Combination no.	Value of α, β	Type of problem	Upper limit of ε	Lower limit of ε
1	0.1, 0.3	Non-convex	0.8	1.8
2	0.1, 0.6	Convex	1.2	1.8
3	0.2, 0.1	Non-convex	0.5	1.3
4	0.2, 0.3	Non-convex	0.5	1.3
5	0.2, 0.5	Convex	0.8	1.3
6	0.2, 0.6	Convex	1.2	1.5
7	0.6, 0.3	Non-convex	0.8	1.8
8	0.6, 0.6	Non-convex	1.2	1.8

Lines 15–20 describe the exploratory moves algorithm, whereas lines 22–25 describe the step updating algorithm.

Algorithm 2: PS applied to NCMCS problem

1: **Input:** Δ_1, P_1
2: $p \leftarrow 1$
3: **Initialization:** *Choose* $\varepsilon_1, \sigma_1, \boldsymbol{\lambda}_1, \boldsymbol{\varrho}_s \in \mathcal{R}^{2K}$, $\theta \in \mathcal{Q}$, $\lambda \in \mathcal{Z}$, $0 < \theta < 1$, and $\lambda \ge 1$
4: **while** $p \le MaxIter_1$ **do**
5: *Starting from* $\boldsymbol{\varrho}_s$, *find an unconstrained local* minimizer $\boldsymbol{\varrho}_p = \min_{\boldsymbol{\varrho}} L_a(\boldsymbol{\varrho}_s, \boldsymbol{\lambda}_p; \sigma_p)$ *as follows*:
6: $q \leftarrow 1$
7: $\boldsymbol{\varrho}_1 \leftarrow \boldsymbol{\varrho}_s$
8: **while** $q \le MaxIter$ **do**
9: *if* $q \ge 1$, *then*
Check for convergence:
10: *if* $((\|L_a(\boldsymbol{\varrho}_q, \boldsymbol{\lambda}_p; \sigma_p) - L_a(\boldsymbol{\varrho}_{q-1}, \boldsymbol{\lambda}_p; \sigma_p)\|_2^2)/(\|L_a(\boldsymbol{\varrho}_q, \boldsymbol{\lambda}_p; \sigma_p)\|_2^2) \le \delta)$, *then* return
11: *end if*
12: *Evaluate the objective function* $L_a(\boldsymbol{\varrho}_q, \boldsymbol{\lambda}_p; \sigma_p)$
13: $i \leftarrow 1$
14: $\boldsymbol{s}_q \leftarrow 0$, $\rho_q \leftarrow 0$, $\nu \leftarrow L_a(\boldsymbol{\varrho}_q, \boldsymbol{\lambda}_p; \sigma_p)$
15: **while** $i \le \widetilde{p}$ **do**
16: $\boldsymbol{s}_q^i \leftarrow \boldsymbol{s}_q + \Delta_q \boldsymbol{p}_q^i$ *and* $\boldsymbol{\varrho}_q^i \leftarrow \boldsymbol{\varrho}_q + \boldsymbol{s}_q^i$. *Evaluate* $L_a(\boldsymbol{\varrho}_q^i, \boldsymbol{\lambda}_p; \sigma_p)$
17: *If* $L_a(\boldsymbol{\varrho}_q^i, \boldsymbol{\lambda}_p; \sigma_p) < \nu$, *then* $\rho_q \leftarrow L_a(\boldsymbol{\varrho}_q, \boldsymbol{\lambda}_p; \sigma_p) - L_a(\boldsymbol{\varrho}_q^i, \boldsymbol{\lambda}_p; \sigma_p)$, $\nu \leftarrow L_a(\boldsymbol{\varrho}_q^i, \boldsymbol{\lambda}_p; \sigma_p)$, *and* $\boldsymbol{s}_q \leftarrow \boldsymbol{s}_q^i$
18: *else*
$\boldsymbol{s}_q^i \leftarrow \boldsymbol{s}_q - \Delta_q \boldsymbol{p}_q^i$, and $\boldsymbol{\varrho}_q^i \leftarrow \boldsymbol{\varrho}_q + \boldsymbol{s}_q^i$. *Evaluate* $L_a(\boldsymbol{\varrho}_q^i, \boldsymbol{\lambda}_p; \sigma_p)$. *If* $L_a(\boldsymbol{\varrho}_q^i, \boldsymbol{\lambda}_p; \sigma_p) < \nu$, *then* $\rho_q \leftarrow L_a(\boldsymbol{\varrho}_q, \boldsymbol{\lambda}_p; \sigma_p) - L_a(\boldsymbol{\varrho}_q^i, \boldsymbol{\lambda}_p; \sigma_p)$, $\nu \leftarrow L_a(\boldsymbol{\varrho}_q^i, \boldsymbol{\lambda}_p; \sigma_p)$, *and* $\boldsymbol{s}_q \leftarrow \boldsymbol{s}_q^i$.
19: *end if*
20: **end while**
21: $\rho_q \leftarrow L_a(\boldsymbol{\varrho}_q, \boldsymbol{\lambda}_p; \sigma_p) - L_a(\boldsymbol{\varrho}_q + \boldsymbol{s}_q, \boldsymbol{\lambda}_p; \sigma_p)$
22: *If* $\rho_q > 0$, *then* $\boldsymbol{\varrho}_{q+1} \leftarrow \boldsymbol{\varrho}_q + \boldsymbol{s}_q$, $\Delta_{q+1} \leftarrow \lambda\Delta_q$
23: *else* $\boldsymbol{\varrho}_{q+1} \leftarrow \boldsymbol{\varrho}_q$, $\Delta_{q+1} \leftarrow \theta\Delta_q$
24: *end if*
25: **end while**
26: $\boldsymbol{\varrho}_p \leftarrow \boldsymbol{\varrho}_q$.
27: *If* $(\boldsymbol{\varrho}_p, \boldsymbol{\lambda}_p)$ *is a Karush–Kuhn–Tucker pair, then stop.*
28: *Choose a penalty parameter* $\sigma_{p+1} \in (0, \sigma_p]$.
29: $\boldsymbol{\lambda}_{p+1} \leftarrow \max(0, \boldsymbol{\lambda}_p + (2/\sigma_p)C(\boldsymbol{\varrho}_p))$.
30: $\boldsymbol{\varrho}_s \leftarrow \boldsymbol{\varrho}_p$, $p \leftarrow p + 1$ *and go to Step 5*
31: **end while**

C. Proposed Solution: PSMI

PS has better performance compared with other algorithms; however, it can be sensitive to initial points as it starts searching for the solution in the vicinity of the initial points. As a result, it can sometimes have irregular performance. To compensate for this irregular performance, a two-step PS algorithm is proposed: In the first step, N_s sets of random input points are selected between an upper and a lower bound, and the solutions of the optimization problem are calculated using these input points. By giving a range of points, a solution near the global optimum point can be calculated. The objective function is evaluated at all the solution points. In the second step, the set of points that gives the best (maximum) value of the objective function is chosen as input to the PS algorithm. The PS algorithm with multiple input (PSMI) algorithm is described by Algorithm 3.

Algorithm 3: Multiple input PS algorithm for NCMCS problem

Initialization: Generate N_s **set of starting points randomly between given lower** and **upper bounds**
Solve the optimization problem using all the sets of starting points
Select the set of points $\hat{\boldsymbol{\varrho}}$ *that gives the minimum value of the objective function*
$\boldsymbol{\varrho}_s \leftarrow \hat{\boldsymbol{\varrho}}$
Solve using Algorithm 2

IV. Simulation Results

Here, a comparison between the proposed PS-based solution and the existing solution is proposed. The proposed method can give better throughput versus interference. A multiband collaborative system consisting of two CRs is considered, i.e., $M = 2$. The channel is divided in eight subbands, i.e., $K = 8$, and hundred measurements are taken, i.e., $N = 100$. The SNR is chosen as -3 dB. These parameters are commonly used in the existing literature. The maximum throughput vector $\boldsymbol{r} = [356, 327, 972, 806, 755, 68, 720, 15]$ kb/s and the cost vector $\boldsymbol{c} = [0.71, 5.95, 3.91, 4.21, 0.44, 2.03, 0.58, 2.85]$ are used in the simulations. The channel gain vectors for the two systems over all the subbands are the following: $\boldsymbol{G}_1 = [0.17, 0.21, 0.27, 0.14, 0.37, 0.38, 0.49, 0.33]$ and $\boldsymbol{G}_2 = [0.21, 0.17, 0.21, 0.21, 0.17, 0.43, 0.15, 0.35]$. Optimization is carried out using different combinations of α and β that are given in Table II: There are three combinations that lead to a convex optimization problem, whereas the remaining combinations lead to nonconvex optimization problems. The values of ε, i.e., the maximum allowed cumulative interference, were varied with a step size of 0.1. The limits of ε are given in Table II for different combinations of α and β.

Comparison is carried out between GA with random initial points as inputs, PS with random initial points as inputs, and PSMI with random inputs. The results of GA are summed over 200 trials. The number of different sets used for the first stage of the PSMI is $N_s = 100$, i.e., hundred different values of weight and threshold vectors were generated with uniform random distribution between the upper and lower respective limits. The points were used as input to solve the optimization problem. The points that give the maximum throughput were used as input to the PS algorithm.

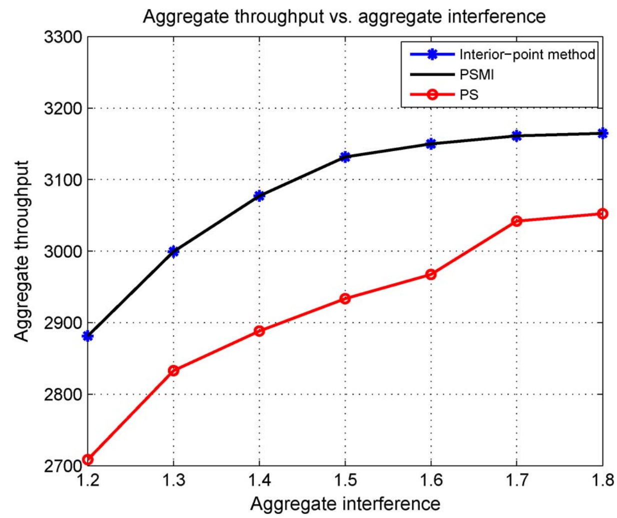

Fig. 4. Comparison of PS and PSMI with the interior-point method for $\alpha = 0.1$, $\beta = 0.6$, convex case.

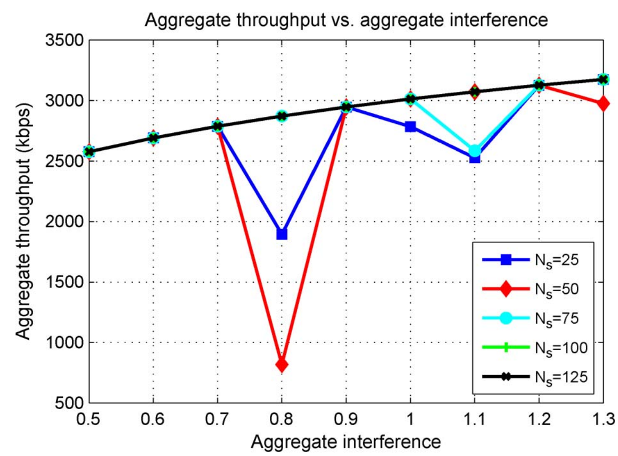

Fig. 5. Performance of PSMI with uniformly distributed input points and varying N_s for $\alpha = 0.2$, $\beta = 0.1$, nonconvex case.

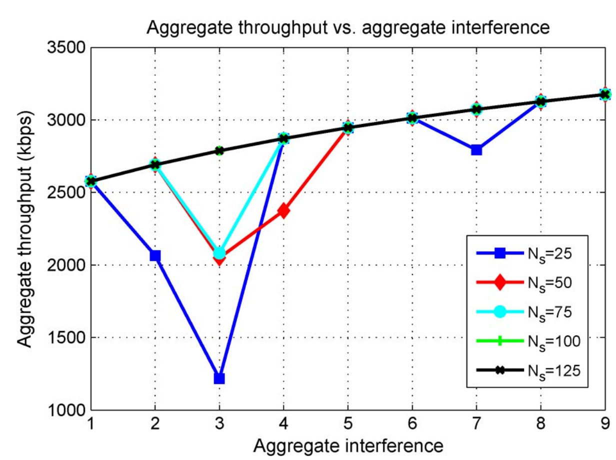

Fig. 6. Performance of PSMI with normally distributed input points and varying N_s for $\alpha = 0.2$, $\beta = 0.1$, nonconvex case.

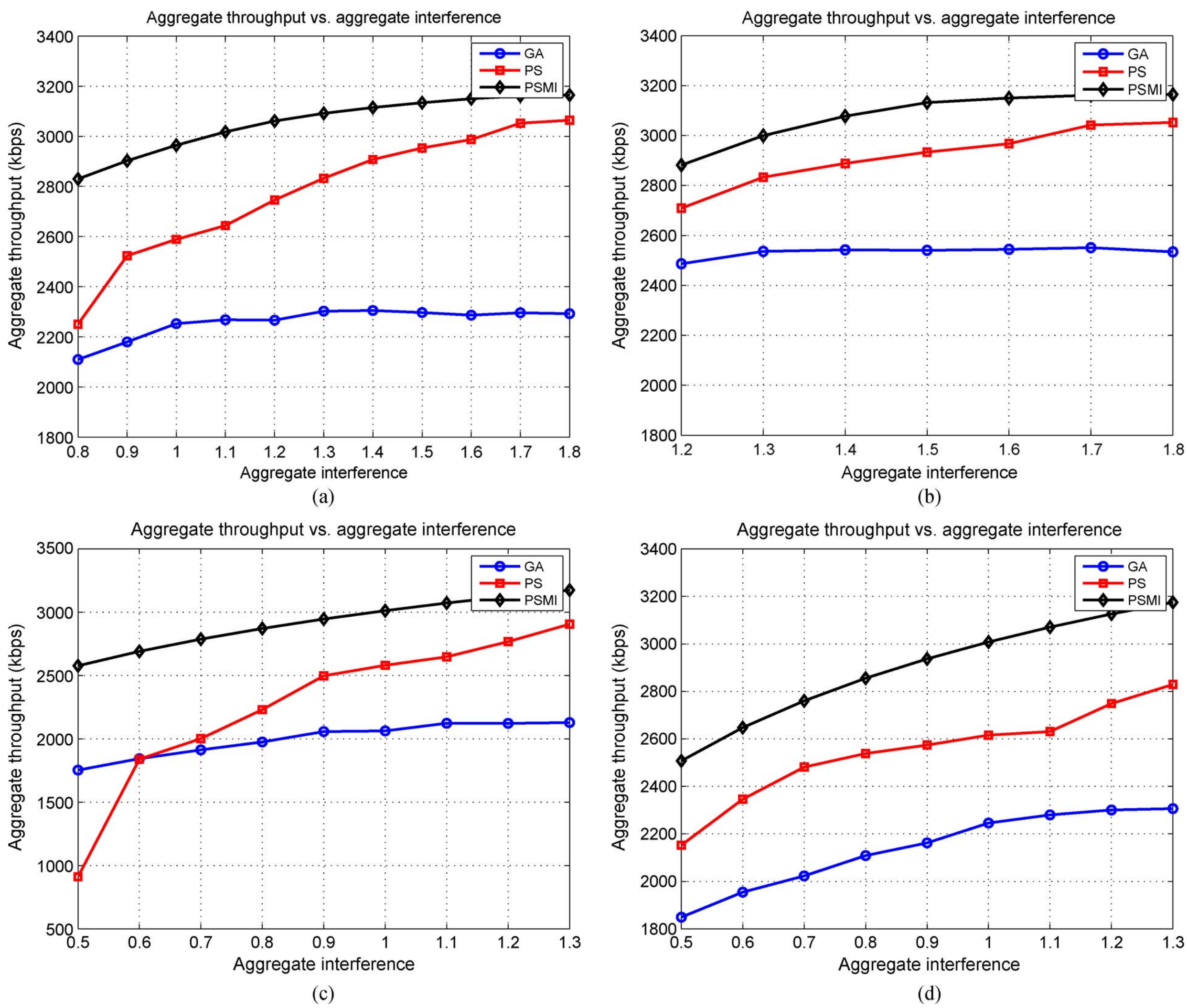

Fig. 7. Cumulative throughput versus interference. (a) $\alpha = 0.1, \beta = 0.3$, nonconvex case. (b) $\alpha = 0.1, \beta = 0.6$, convex case. (c) $\alpha = 0.2, \beta = 0.1$, nonconvex case. (d) $\alpha = 0.2, \beta = 0.3$, nonconvex case.

For simulations, the initial values of θ and λ are 0.5 and 1, respectively. These initial values were varied, and the results and the computation time were seen as independent of the initial values. First, a comparison of the proposed method with the interior-point method for convex case is shown. In the convex case, the solution is guaranteed, and the closeness of solutions based on the proposed method with the reference solution obtained by the interior-point method is compared. The results are shown in Fig. 4. It can be seen that, although the PS-based solution is close to the reference solution, the PSMI-based solution is overlapping with the reference solution. This shows the effectiveness of the proposed PSMI method.

Next, the dependence of the number of different sets N_s on the performance of PSMI is shown. N_s is varied from 25 to 125 in a step size of 25; the values of α and β are 0.2 and 0.1, respectively. The results are shown in Fig. 5. It can be seen that the througput continuously increases as the interference increases with values of $N_s = 100$ and $N_s = 125$, whereas for lower values, the results are irregular. This is so as a higher value of N_s means that there are more chances of finding a solution near the global solution in the first step of the PSMI, and hence, the performance is less erratic. The initial distribution is selected as uniform; then, the initial points can be limited between upper and lower limits. Results are also shown with initial normally distributed threshold values in Fig. 6, where the mean of the distribution is the average of lower and upper limits, and the standard deviation is chosen such that most of the points will fall between the lower and upper limits. The initial weights are distributed using uniform distribution as then, they can be limited between 0 and 1. It can be seen that a higher number of points are still needed to get a reasonable performance. In the rest of this section, we use uniformly distributed initial values with $N_s = 100$.

The results of cumulative throughput versus cumulative interference are shown in Figs. 7(a)–8(d) for different values of α and β. The following observations can be made.

- PS outperforms GA, whereas the proposed PSMI outperforms PS. The method can achieve greater throughput at a lower interference.
- The cumulative throughput in nonconvex systems is higher for a given level of cumulative interference, compared with the convex systems. This is true for the all the approaches.
- The difference in cumulative throughput value at a particular interference value between PSMI and GA is higher

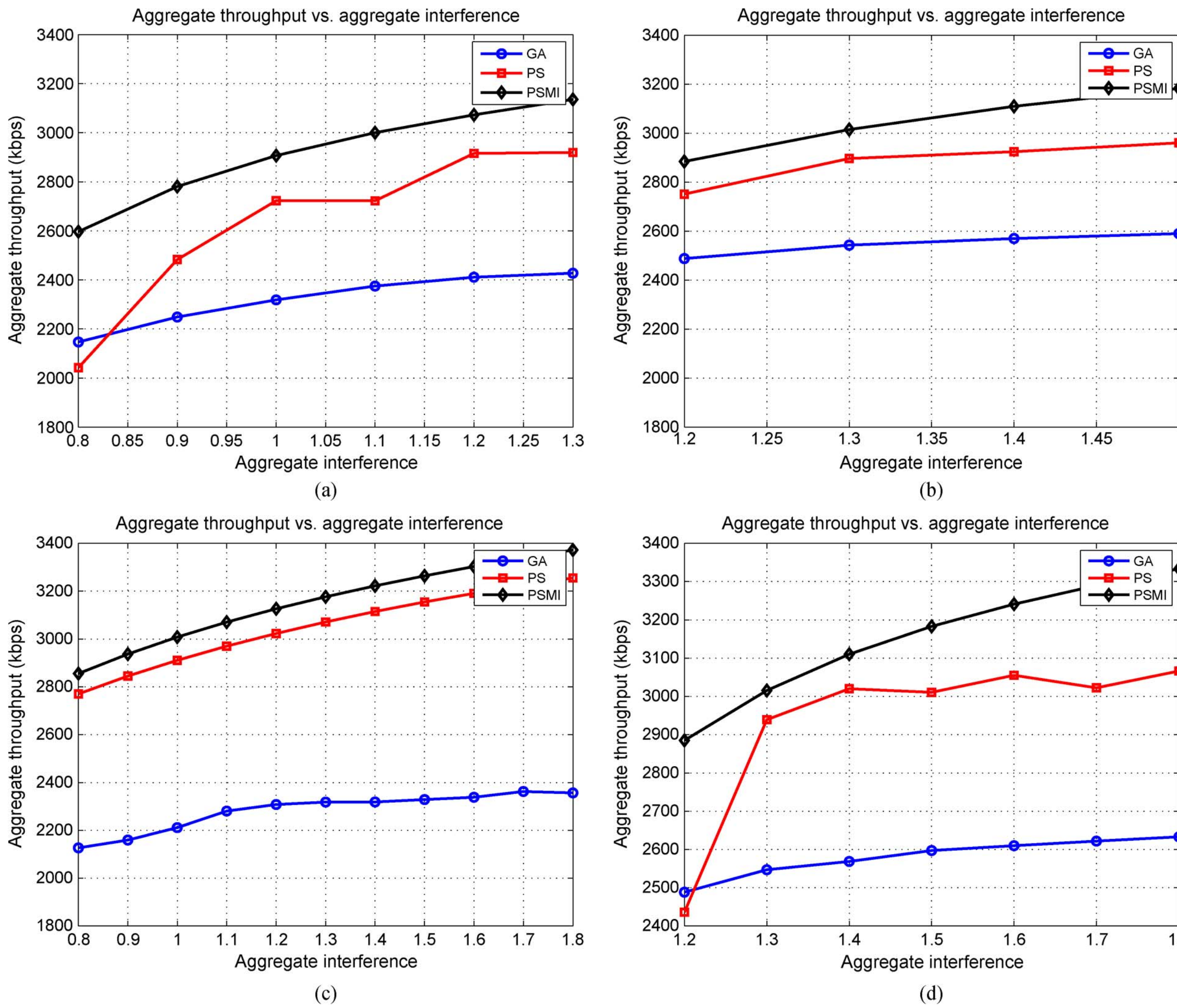

Fig. 8. Cumulative throughput versus interference. (a) $\alpha = 0.2$, $\beta = 0.5$, convex case. (b) $\alpha = 0.2$, $\beta = 0.6$, convex case. (c) $\alpha = 0.6$, $\beta = 0.3$, nonconvex case. (d) $\alpha = 0.6$, $\beta = 0.6$, nonconvex case.

for nonconvex systems. This can be particularly noticed in Figs. 7(a), (c), and (d) and 8(c), where the difference is approximately 700 kb/s, compared with Figs. 7(b) and 8(a), where this difference is around 400 kb/s. This shows that our algorithm offers better solution for the nonconvex case.

- The PS algorithm is sensitive to the initial inputs. This can be seen through the sometimes irregular behavior of cumulative throughput versus cumulative interference obtained using the PS algorithm: It is shown in Figs. 7(c) and 8(a) and (d) that the cumulative throughput suddenly increases. The reason is that the randomly selected random points used as input do not always provide the optimum solution. However, with the proposed method, the cumulative throughput versus interference always follows the increasing trend.

Next, a plot of the number of objective function evaluations versus different combinations of α and β and $\epsilon = 1.3$ is shown in Fig. 9. It can be seen that the proposed method requires less function evaluations compared with GA.

Results for $1 - P_d$ and $1 - P_f$ calculated using the weights and threshold obtained from all the three approaches at $\alpha = 0.2$,

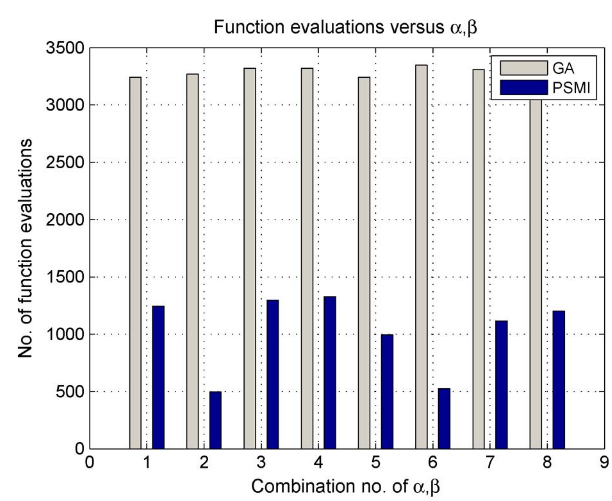

Fig. 9. Number of function evaluations versus different combinations of α, β. Combination numbers correspond to Table II.

$\beta = 0.3$, and $\varepsilon = 1.3$ are shown in Fig. 10(a)–(f). The following observations can be made.

- It is shown in Fig. 10(e) that subbands 2, 6, and 8 give lower values compared with Fig. 10(c). The reason is

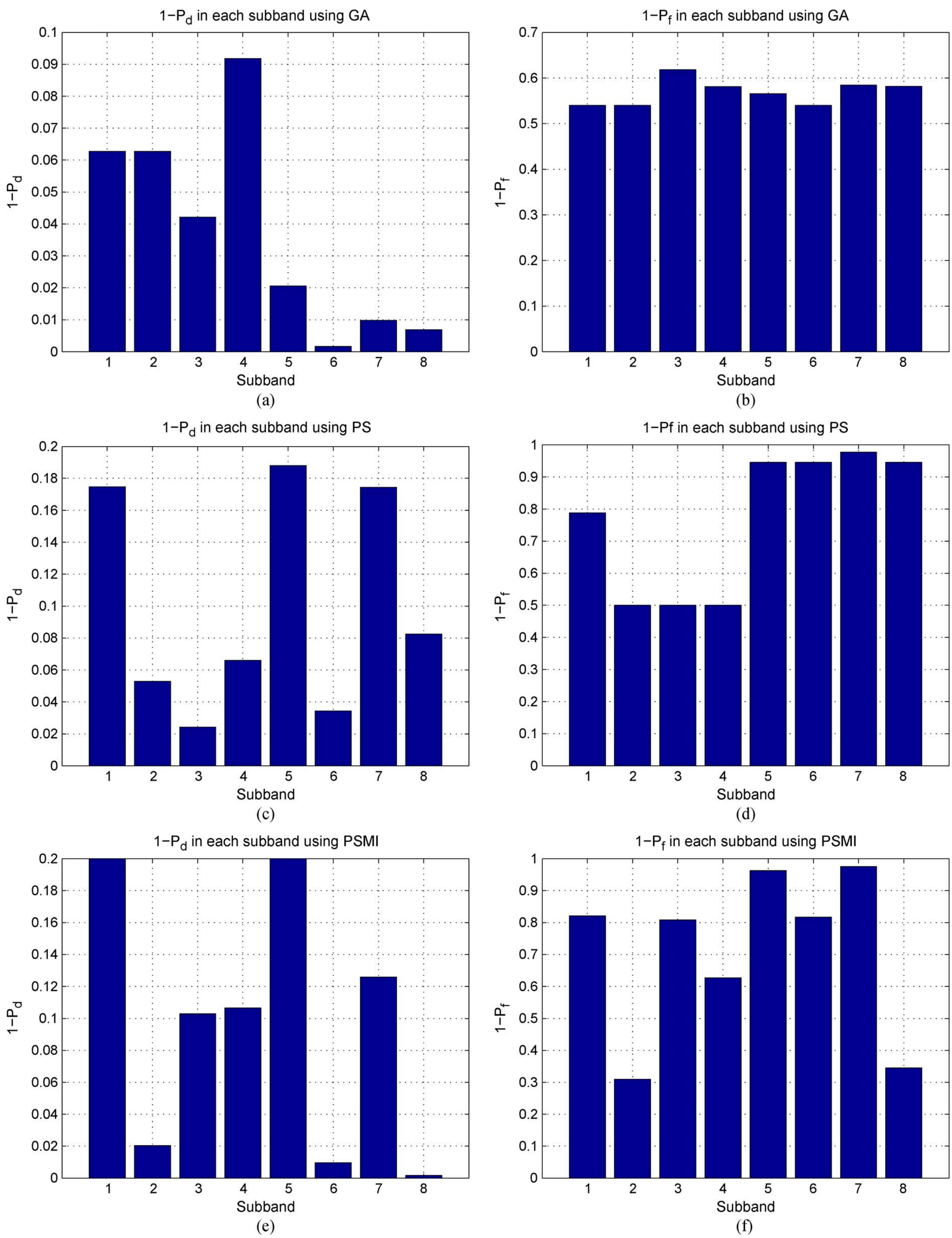

Fig. 10. $1-P_d$ and $1-P_f$ for $\varepsilon=1.3$. (a) $1-P_d$ using GA, $\alpha=0.2, \beta=0.3, \varepsilon=1.3$. (b) $1-P_f$ using GA, $\alpha=0.2, \beta=0.3, \varepsilon=1.3$. (c) $1-P_d$ using PS, $\alpha=0.2, \beta=0.3, \varepsilon=1.3$. (d) $1-P_f$ using PS, $\alpha=0.2, \beta=0.3, \varepsilon=1.3$. (e) $1-P_d$ using PSMI, $\alpha=0.2, \beta=0.3, \varepsilon=1.3$. (f) $1-P_f$ using PSMI, $\alpha=0.2, \beta=0.3, \varepsilon=1.3$.

that these subbands have higher costs; consequently, the values of optimized weights and thresholds should be such that $1-P_d$ has lower values. This can be explained by the fact that as the cost is higher in these subbands, the value of $1-P_d$ should be lower to reduce interference. This is evident from (12). Note that this is also true for Fig. 10(a), except for subband 6, where the value is lower. However, the reason for this lower value of $1-P_d$ in Fig. 10(a) is that the solution obtained using GA is less optimal.

- It is shown in Fig. 10(f) that subbands 3–5 give higher values compared with Fig. 10(b) and (d). As it can be noted from (13), in order to achieve a higher cumulative throughput, those bands that have higher values of maximum achievable throughput should also have a higher value of $1 - P_f$, so that the cumulative throughput becomes higher. It is evident that the proposed approach is able to allocate a higher value at a band with maximum achievable output.

V. Conclusion

In this paper, a solution based on PS algorithm has been applied for solving NCMCS problem. A two-step PS-based solution is presented, which is called PSMI. The first step of PSMI solves the optimization problem using randomly generated sets of points as input. In the second step, the set of points that gives the maximum throughput is chosen as input to the PS algorithm. Numerical examples show the improvement of the proposed method over existing algorithms. The proposed method gets consistent results, gives better cumulative throughput, decreases the probability of false alarm, increases the probability of detection, and uses less function evaluations compared with the GA.

References

[1] "Federal communication commission spectrum policy task force," Washington, DC, USA, Rep. ET Docket no. 02-135, 2002.

[2] S. Haykin, "Cognitive radio: Brain-empowered wireless communications," *IEEE J. Sel. Areas Commun.*, vol. 23, no. 2, pp. 201–220, Feb. 2005.

[3] M. Hoyhtya, J. Kyrolainen, A. Hulkkonen, J. Ylitalo, and A. Roivainen, "Application of cognitive radio techniques to satellite communication," in *Proc. IEEE DYSPAN*, 2012, pp. 540–551.

[4] D. Raychaudhuri and N. Mandayam, "Frontiers of wireless and mobile communications," *Proc. IEEE*, vol. 100, no. 4, pp. 824–840, Apr. 2012.

[5] P. Phunchongharn, E. Hossain, D. Niyato, and S. Camorlinga, "A cognitive radio system for e-health applications in a hospital environment," *IEEE Wireless Commun.*, vol. 17, no. 1, pp. 20–28, Feb. 2010.

[6] S. Chang, K. Nagothu, B. Kelley, and M. Jamshidi, "A beamforming approach to smart grid systems based on cloud cognitive radio," *IEEE Syst. J.*, vol. 8, no. 2, pp. 461–470, Jun. 2014.

[7] T. Kolda, R. Lewis, and V. Torczon, "Optimization by direct search: New perspectives on some classical and modern methods," *SIAM Rev.*, vol. 45, no. 3, pp. 385–582, 2003.

[8] H. Poor, *An Introduction to Signal Detection and Estimation*. Berlin, Germany: Springer-Verlag, 1994.

[9] S. Enserink and D. Cochran, "A cyclostationary feature detector," in *Proc. 28th Asilomar Conf. Signals, Syst. Comput.*, 1994, pp. 806–810.

[10] S. Kay, *Fundamental of Statistical Signal Processing: Volume II: Detection Theory*. Englewood Cliffs, NJ, USA: Prentice-Hall, 1998.

[11] S. Shellhammer, S. Shankar, R. Tandra, and J. Tomcik, "Performance of power detector sensors of DTV signals in IEEE 802.22 WRANs," in *Proc. TAPAS*, 2006, pp. 1–9.

[12] H. Urkowitz, "Energy detection of unknown deterministic signals," *Proc. IEEE*, vol. 55, no. 4, pp. 523–531, Apr. 1967.

[13] D. Cabric, A. Tkachenko, and R. Brodersen, "Experimental study of spectrum sensing based on energy detection and network cooperation," in *Proc. TAPAS*, 2006, pp. 1–8.

[14] S. Mishra, A. Sahai, and R. Brodersen, "Cooperative sensing among cognitive radios," in *Proc. IEEE ICC*, 2006, pp. 1658–1663.

[15] I. Akyildiz, B. Lo, and R. Balakrishnan, "Cooperative spectrum sensing in cognitive radio networks: A survey," *J. Phys. Commun.*, vol. 4, no. 1, pp. 40–62, Mar. 2011.

[16] E. Peh and Y. Liang, "Optimization for cooperative sensing in cognitive radio networks," in *Proc. IEEE WCNC*, 2007, pp. 27–32.

[17] P. Qihang, Z. Kun, W. Jun, and L. Shaoqian, "A distributed spectrum sensing scheme based on credibility and evidence theory in cognitive radio context," in *Proc. IEEE Int. Symp. Pers., Indoor, Mobile Radio Commun.*, 2006, pp. 1–5.

[18] Z. Quan, S. Cui, A. Sayed, and H. Poor, "Optimal multiband joint detection for spectrum sensing in cognitive radio networks," *IEEE Trans. Signal Process.*, vol. 57, no. 3, pp. 1128–1140, Mar. 2009.

[19] Z. Quan, S. Cui, H. Poor, and A. Sayed, "Collaborative wideband sensing for cognitive radios," *IEEE Signal Process. Mag.*, vol. 25, no. 6, pp. 60–73, Nov. 2008.

[20] T. Zhang, Y. Wu, K. Lang, and D. Tsang, "Optimal scheduling of cooperative spectrum sensing in cognitive radio networks," *IEEE Syst. J.*, vol. 4, no. 4, pp. 535–549, Dec. 2010.

[21] A. Sahai and D. Cabric, "A tutorial on spectrum sensing: Fundamental limits and practical challenges," *Tutorial IEEE DySPAN*, Baltimore, MD, USA, 2005.

[22] Z. Tian and G. B. Giannakis, "A wavelet approach to wideband spectrum sensing for cognitive radios," in *Proc. 1st CROWNCOM*, 2006, pp. 1–5.

[23] Y. Hur, J. Park, W. Woo, K. Lim, C.-H. Lee, H. Kim, and J. Laskar, "A wideband analog multi-resolution spectrum sensing technique for cognitive radio systems," in *Proc. IEEE ISCAS*, 2006, pp. 4090–4092.

[24] X.-S. Yang, *Introduction to Mathematical Optimization: From Linear Programming to Metaheuristics*. Cambridge, U.K.: Cambridge International Science Publishing, 2009.

[25] M. Saeedzarandi and P. Azmi, "Cooperative multiband joint detection in cognitive radio networks using artificial immune system," *Ann. Telecommun.*, vol. 68, no. 3/4, pp. 239–246, Apr. 2013.

[26] Y. Ma and D. Liu, "Optimal cooperative spectrum sensing in cognitive radio with Taguchi method," in *Proc. IEEE VTC*, 2012, pp. 1–5.

[27] M. Sanna and M. Murroni, "Optimization of non-convex multiband cooperative sensing with genetic algorithms," *IEEE J. Sel. Topics Signal Process.*, vol. 5, no. 1, pp. 87–96, Feb. 2011.

[28] V. Torczon, "Pattern search methods for nonlinear optimization," *SIAG/OPT Views News*, no. 6, pp. 7–11, 1995.

[29] S. Huang, H. Chen, Y. Zhang, and H.-H. Chen, "Sensing-energy tradeoff in cognitive radio networks with relays," *IEEE Syst. J.*, vol. 4, no. 4, pp. 68–76, Mar. 2012.

[30] E. Elbeltagi, T. Hegazy, and D. Grierson, "Comparison among five evolutionary-based optimization algorithms," *Adv. Eng. Inf.*, vol. 19, no. 1, pp. 43–53, Jan. 2005.

[31] R. Lewis, V. Torczon, and M. Trosset, "Why pattern search works," *Optima*, no. 59, pp. 1–7, Oct. 1998.

[32] M. Pedersen, "Tuning and simplifying heuristical optimization," Ph.D. dissertation, Univ. Southampton, Southampton, U.K., 2010.

[33] Y. Labbi and D. Attous, "A hybrid particle swarm optimization and pattern search method to solve the economic load dispatch problem," *Int. J. Syst. Assur. Eng. Manag.*, Jul. 26, 2013, DOI: 10.1007/s13198-013-0186-1, to be published.

[34] J. Vasconcelos, J. Ramıacute;rez, R. Takahashi, and R. Saldanha, "Improvements in genetic algorithms," *IEEE Trans. Magn.*, vol. 37, no. 5, pp. 3414–3417, Sep. 2001.

[35] P. Pardalos and M. Resende, *Handbook of Applied Optimization*. London, U.K.: Oxford Univ. Press, 2002.

[36] V. Torczon, "On the convergence of pattern search algorithms," *Siam J. Optim.*, vol. 7, no. 1, pp. 1–25, 1997.

[37] Z. Quan, W. Ma, S. Cui, and A. Sayed, "Optimal linear fusion for distributed spectrum sensing via semidefinite programming," *IEEE Trans. Signal Process.*, vol. 58, no. 4, pp. 2431–2436, Apr. 2010.

Ahmed Shaharyar Khwaja received the B.Sc. degree in electronic engineering from Ghulam Ishaq Khan Institute of Engineering Sciences and Technology, Topi, Pakistan, and the Ph.D. and M.Sc. degrees in signal processing and telecommunications from the University of Rennes 1, Rennes, France.

He is currently a Postdoctoral Research Fellow with the WINCORE Lab, Ryerson University, Toronto, ON, Canada. His research interests include compressed sensing, remote sensing, and optimization problems in wireless communication systems.

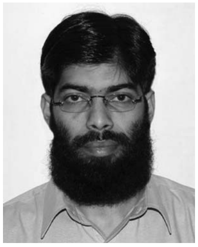

Muhammad Naeem received the B.S. and M.S. degrees in electrical engineering from the University of Engineering and Technology Taxila, Taxila, Pakistan, in 2000 and 2005, respectively, and the Ph.D. degree from Simon Fraser University, Burnaby, BC, Canada, in 2011.

From 2000 to 2005, he was a Senior Design Engineer in the Design Department with Comcept (Pvt) Ltd., Islamabad, Pakistan. From 2012 to 2013, he was a Postdoctoral Research Associate with the WINCORE Lab, Ryerson University, Toronto, ON, Canada. Since August 2013, he has been an Assistant Professor with the Department of Electrical Engineering, COMSATS Institute of Information Technology, Wah Cantt, Pakistan, and a Research Associate with the WINCORE Lab. He participated in the design and development of smart-card-based Global System for Mobiles and code-division multiple-access pay phones. He is also a Microsoft Certified Solution Developer. His research interests include optimization of wireless communication systems, nonconvex optimization, resource allocation in cognitive radio networks, and approximation algorithms for mixed-integer programming in communication systems.

Dr. Naeem has been a recipient of Natural Sciences and Engineering Research Council Canada Graduate Scholarship.

Alagan Anpalagan received the B.A.Sc., M.A.Sc., and Ph.D. degrees in electrical engineering from the University of Toronto, Toronto, ON, Canada.

In 2001, he joined the Department of Electrical and Computer Engineering, Ryerson University, Toronto, where he was promoted to Full Professor in 2010. He served the department as the Graduate Program Director (2004–2009) and the Interim Electrical Engineering Program Director (2009–2010). He directs a research group working on radio resource management and radio access and networking areas within the WINCORE Lab. During his sabbatical (2010–2011), he was a Visiting Professor with Asian Institute of Technology and a Visiting Researcher with Kyoto University, Kyoto, Japan. His industrial experience includes working at Bell Mobility, Nortel Networks, and IBM Canada. He has coauthored three edited books, namely, *Design and Deployment of Small Cell Networks* (Cambridge University Press, 2014), *Routing in Opportunistic Networks* (Springer, 2013), and *Handbook on Green Information and Communication Systems* (Academic Press, 2012). His current research interests include cognitive radio resource allocation and management, wireless cross-layer design and optimization, cooperative communication, machine-to-machine communication, small cell networks, and green communications technologies.

Dr. Anpalagan has served as an Associate Editor of the IEEE *Communications Surveys & Tutorials* since 2012 and Springer *Wireless Personal Communications* since 2009. He was an Associate Editor of the IEEE Communications Letters in 2010–2013 and an Editor of EURASIP *Journal of Wireless Communications and Networking* in 2004–2009. He also served as a Guest Editor for two EURASIP special issues on Radio Resource Management in 3G+ Systems in 2006 and Fairness in Radio Resource Management for Wireless Networks in 2008 and MONET special issues on Green Cognitive and Cooperative Communication and Networking in 2012. He served as the Technical Program Committee Cochair for the IEEE WPMC 2012 Wireless Networks, the IEEE PIMRC 2011 Cognitive Radio and Spectrum Management, the IEEE IWCMC 2011 Workshop on Cooperative and Cognitive Networks, the IEEE CCECE 2004/2008, and the WirelessCom 2005 Symposium on Radio Resource Management. He served as the IEEE Canada Central Area Chair in 2013–2014, the IEEE Toronto Section Chair in 2006–2007, the ComSoc Toronto Chapter Chair in 2004–2005, and the IEEE Canada Professional Activities Committee Chair in 2009–2011. He was the recipient of the Dean's Teaching Award in 2011; the Faculty Scholastic, Research and Creativity Award in 2010; and the Faculty Service Award in 2010 at Ryerson University. He has completed a course on Project Management for Scientists and Engineers from the University of Oxford Continuing Professional Development Center. He is a Registered Professional Engineer in the province of Ontario, Canada.